

Properties of Positive Resists. III. The Dissolution Behavior of Poly(methyl Methacrylate-co-Maleic Anhydride)

RASHMI K. DRUMMOND,* GAIL L. BOYDSTON,[†] and
NIKOLAOS A. PEPPAS,[‡] *School of Chemical Engineering,
Purdue University West Lafayette, Indiana 47907*

Synopsis

The dissolution characteristics of model positive resists were investigated through the use of various copolymers of methyl methacrylate and maleic anhydride. Dissolution in methyl ethyl ketone was found to be dependent on the radiation dose and on the composition of the copolymers. The Lee–Peppas dissolution model was used to calculate important parameters of this dissolution process. It was shown that the overall dissolution rate was initially controlled by the swelling process whereas the true disentanglement/dissolution process predominated during the latter portion of the overall phenomenon. In addition, the thickness of the formed gel layer was a function of the square root of time.

INTRODUCTION

Development of positive resists has been a subject of significant interest in the microelectronic industry in the past 10 years. Positive resists function because, upon directional irradiation, they are degraded and dissolved, thus forming the basic pattern of an integrated circuit.^{1,2}

It is evident that the dissolution properties of positive resists are instrumental in the development of accurate IC devices with excellent contrast. This problem has been discussed by several investigators including Ouano,^{3–5} Soong,⁶ Rodriguez,^{7,8} and their collaborators. Several models have been proposed and experimental studies have been obtained in recent years to analyze this dissolution process.

In our laboratory, an effort has been undertaken to describe the dissolution of glassy polymers used as positive resists. The previous work in this series,^{9,10} but also more recent work of direct applicability to this field,^{11,12} have shown that the positive resist dissolution process consists of two phenomena: (i) a swelling process with a transition from the glassy to the rubbery state and (ii) a dissolution process of the swollen polymer. As discussed by Harland et al.,¹² depending on the relative velocity of the rubbery transition and the dissolution fronts, the thickness of the gel layer of a swelling film changes with time according to Figure 1. In this figure, an initial rise in gel thickness is observed which is indicative of considerable swelling of the polymer with slower dissolution. Later, the swelling of the gel layer becomes balanced with

*Present address: Kraft General Goods, Glenview, IL 60025.

[†]Present address: Eli Lilly & Company, Indianapolis, IN 46250.

[‡]Corresponding author.

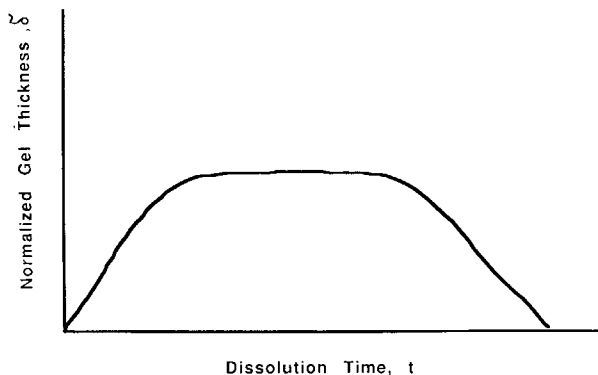


Fig. 1. Typical plot of the dependence of normalized gel thickness δ on dissolution time t for a positive resist.

its dissolution and a constant gel thickness is observed. The final step in the dissolution process is described by a decrease in gel thickness when the dissolution rate overcomes the swelling rate.

In the present work, we offer further evidence of the influence of copolymer composition and irradiation on the dissolution characteristics of model positive resists.

EXPERIMENTAL

Random copolymers of methyl methacrylate (MMA) with maleic anhydride (MAH) were prepared by solution polymerization. In a typical experiment, vacuum-distilled methyl methacrylate was mixed with maleic anhydride (both obtained from Aldrich Chemical Co., Milwaukee, WI), and 0.005 mol % of benzoyl peroxide was added as an initiator. To this mixture, methanol was added as a solvent at a volumetric ratio of approximately 4:5. The copolymerization reaction was carried out at 50°C for 48 h followed by 24 h at 70°C in polypropylene vials. Since the conversion was virtually 100%, the final copolymer composition was the same as that of the comonomer feed. Copolymers containing, 0.20, 0.30, 0.40, 0.50, 0.60, 0.70, and 0.80 molar fractions of MMA (on a dry basis) were prepared in addition to pure PMMA. The final copolymers were random because the reactivity ratios¹³ were $r_1 = 6.7$ and $r_2 = 0.02$.

The resulting methanol-swollen cylindrical samples were cut with a diamond-edge lathe in thin disks of 14 mm diameter and 2.2 mm thickness. These were dried in a vacuum oven until constant weight was obtained for several days and further cut radially to give thin slabs.

All copolymer samples were irradiated with γ -irradiation in a Co⁶⁰ unit with a dose rate of 2,344 rad/min for a total of 4 or 10 Mrad. The molecular weight distribution of unirradiated and irradiated P(MMA-co-MAH) samples was determined by gel permeation chromatography, as discussed before.¹⁰

Solubility studies were performed in a wide range of organic and polar solvents, including water, methanol, ethanol, isopropanol, 1-octanol, benzyl alcohol, 1,3-butanediol, acetone, methyl ethyl ketone (MEK), cyclohexanone, dimethyl formamide (DMF), dimethyl sulfoxide (DMSO), *n*-heptane, cyclohexane, toluene, dichloromethane, chloroform, and carbon tetrachloride. Small

samples of the various copolymers were placed in test tubes in each solvent and the sample dissolution, swelling or insolubility was judged. Dissolution studies of unirradiated and degraded PMMA and copolymers of P(MMA-co-MAH) with 0.40, 0.60, and 0.80 molar fraction of MMA were performed in MEK, ethanol, and cyclohexanone at 26°C.

RESULTS AND DISCUSSION

Solubility Characteristics of P(MMA-co-MAH)

Solubility studies were conducted to establish the solubility characteristics of P(MMA-co-MAH). To study the effect of copolymer composition on the dissolution properties, copolymers of P(MMA-co-MAH) containing molar fractions of MMA of 0.40, 0.60, and 0.80 were examined. In addition, the effect of irradiation on the solubility properties of the copolymers was studied by examining copolymers with the same compositions which were irradiated at 4 and 10 Mrad. The type of irradiation used does not affect the polymer degradation mechanism.²

Based on these studies, the solubility diagrams for unirradiated P(MMA-co-MAH) with molar fractions of 0.40, 0.60, and 0.80 MMA were constructed by the use of the Hansen analysis¹⁴ and are presented in Figures 2, 3, and 4, respectively. In this analysis, the solubility parameter is given by a 3-dimen-

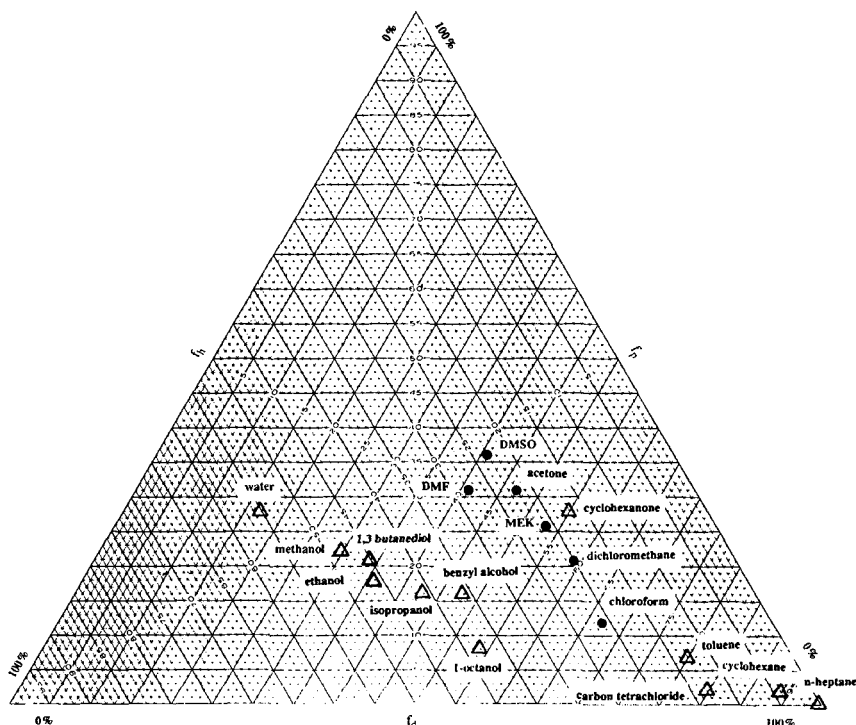


Fig. 2. A mapping of the fractional solubility parameters due to hydrogen bonding, f_h , polar, f_p , and dispersion, f_d , interactions for the dissolution of P(MMA-co-MAH) with 0.40 molar fraction of MMA in various solvents at 26°C: (●) good solvents; (○) solvents that produce swollen gels; (Δ) nonsolvents.

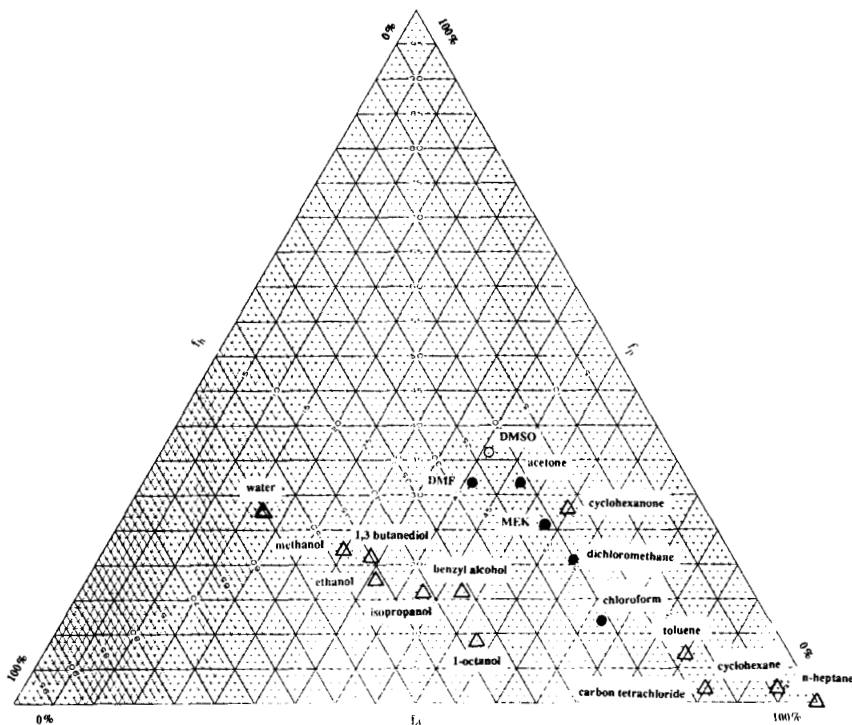


Fig. 3. A mapping of the fractional solubility parameters due to hydrogen bonding, f_h , polar, f_p , and dispersion, f_d , interactions for the dissolution of P(MMA-co-MAH) with 0.60 molar fraction of MMA in various solvents at 26°C: (●) good solvents; (○) solvents that produce swollen gels; (Δ) nonsolvents.

sional equation

$$f^2 = f_d^2 + f_p^2 + f_h^2 \quad (1)$$

Here f_d represents the dispersion contribution, f_p the polar contribution, and f_h the hydrogen bonding contribution to the solubility parameters. Comparison of solubility data in this manner can indicate physical differences between different polymers. The f_h , f_p , and f_d values of the various solvents or nonsolvents were plotted in a triangular diagram based on literature data for the solubility parameters.¹⁵ The filled circles indicate regions of adequate dissolution of the copolymer, the open circles indicate swelling without dissolution, and the triangles represent nonsolvents. In all cases, a region of thermodynamic compatibility was established, within which thermodynamically good solvents could be identified according to their polar, hydrogen bonding, and dispersion interactions with the copolymer.

Although this analysis is subject to operator objectivity, these diagrams indicate the progressive change of the solubility of the copolymer as a function of composition. Varying the composition of the copolymer resulted in changes of the dissolution properties in the presence of four of the solvents studied: toluene, carbon tetrachloride, dimethyl sulfoxide (DMSO), and cyclo-

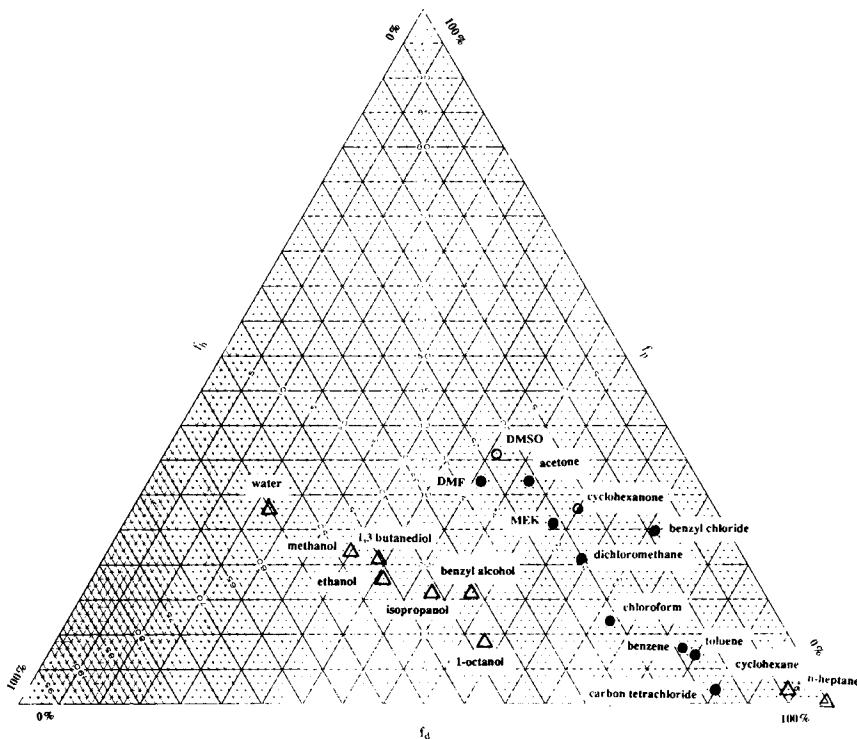


Fig. 4. A mapping of the fraction solubility parameters due to hydrogen bonding, f_h , polar, f_p , and dispersion, f_d , interactions for the dissolution of P(MMA-co-MAH) with 0.80 molar fraction of MMA in various solvents at 26°C: (●) good solvents; (○) solvents that produce swollen gels; (△) nonsolvents.

hexanone. As an example, carbon tetrachloride was a nonsolvent for the copolymers with 0.40 and 0.60 MMA, a solvent which swelled the copolymer with 0.70 MMA and a good solvent for the copolymer with 0.80 MMA. Thus, exposure/development solvents can be identified for each composition.

The greatest effect of irradiation on the solubility properties was observed for P(MMA-co-MAH) samples containing 0.40 MMA. Although cyclohexanone was a nonsolvent for the unirradiated copolymer, it became a solvent for the copolymer irradiated with 4 Mrad. Similarly, benzyl alcohol, which was a nonsolvent for the unirradiated copolymer, was rendered a solvent which swelled the copolymer upon irradiation with 4 Mrad. Copolymers irradiated with 10 Mrad were swollen in cyclohexane and 1-octanol, which were nonsolvents for the corresponding unirradiated copolymers. Finally, benzyl alcohol was a nonsolvent for the unirradiated copolymer and a good solvent for the irradiated (with 10 Mrad) copolymer.

Upon irradiation of P(MMA-co-MAH) containing 0.60 MMA, carbon tetrachloride, which was originally a nonsolvent for the unirradiated copolymer, became a good solvent. This result was observed with copolymers irradiated with both 4 and 10 Mrad. Finally, for P(MMA-co-MAH) with 0.80 MMA, copolymers irradiated with both 4 and 10 Mrad were soluble in cyclohexanone, whereas the unirradiated copolymer only swelled in this liquid.

TABLE I
Change in Solubility Properties of P(MMA-co-MAH) upon Irradiation

Copolymer MMA composition (molar fraction)	Liquid	Liquid in contact with unirradiated copolymer	Radiation dose (Mrad)	Liquid in contact with irradiated copolymer
0.40	Cyclohexanone	Nonsolvent	4	Solvent
	Benzyl alcohol	Nonsolvent	4	Swelling agent
	Cyclohexanone	Nonsolvent	10	Solvent
	Benzyl alcohol	Nonsolvent	10	Solvent
	Cyclohexane	Nonsolvent	10	Swelling agent
	1-Octanol	Nonsolvent	10	Swelling agent
0.60	Carbon tetrachloride	Nonsolvent	4	Solvent
	Carbon tetrachloride	Nonsolvent	10	Solvent
0.80	Cyclohexanone	Swelling agent	4	Solvent
	Benzyl alcohol	Nonsolvent	4	Swelling agent
	Cyclohexanone	Swelling agent	10	Solvent
	Benzyl alcohol	Nonsolvent	10	Solvent

Therefore, upon irradiation P(MMA-co-MAH) degrades so that appropriate solvents for the low molecular weight chains can be found. Furthermore, in positive resist applications of these polymers an irradiated sample can be dissolved by the same solvent which will not affect the unirradiated portion. A thorough presentation of these phenomena is given in Table I.

Polymer Dissolution

Dissolution studies of P(MMA-co-MAH) were performed in MEK at 26°C. Using optical micrography, the thickness of the gel layer formed during the concurrent swelling and dissolution processes was measured and recorded as a function of time. Typical results of the normalized gel thickness δ [the gel (rubbery) layer thickness divided by the initial, unswollen sample thickness], for a copolymer with 0.40 MMA as a function of square root of time are presented in Figure 5.

As predicted by Harland et al.,¹² Lee and Peppas,¹¹ and Parsonage et al.,⁹ an initial rise in normalized gel thickness occurred (in region OA) until a maximum value was attained (at point A). This maximum was followed by a decrease in normalized gel thickness when the dissolution mechanism overcame the swelling process. Because two distinct plateaus could be detected (BC and DE), this example is a clear indication of the existence of different molecular weight chains formed due to irradiation. The portion of the curve between 8 and 13 min (around point A) is the region of major change of the swelling and dissolution rates and has been drawn with a dashed curve.

The normalized thickness versus square root of time for typical P(MMA-co-MAH) samples with 0.60 MMA before irradiation, after 4 and 10 Mrad irradiations are shown in Figures 6, 7, and 8, respectively. For the unirradiated copolymer, no degradation occurred, and swelling was the prominent phenomenon. An initial rise in normalized gel thickness was observed as a function of the square root of time until a plateau was reached.

For the sample irradiated with 4 Mrad, the same type of behavior was seen until a drop after the plateau occurred due to true dissolution. The result of

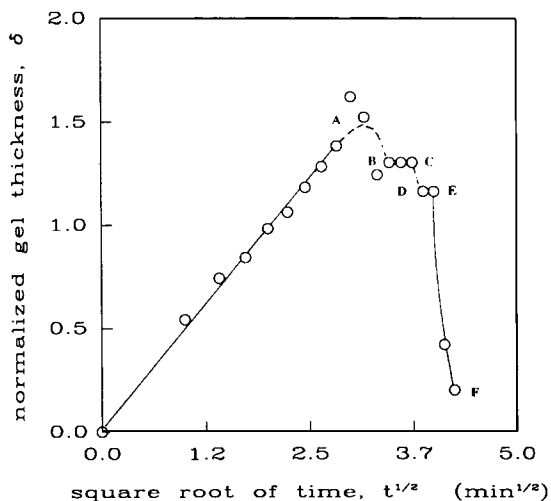


Fig. 5. Normalized gel thickness as a function of the square root of solvent diffusion time for MEK dissolution of P(MMA-co-MAH) slabs containing 0.40 molar fraction of MMA and irradiated with 4 Mrad.

degrading the copolymer by irradiation was that the plateau value of normalized gel thickness was much lower than that of the unirradiated copolymer (compare Figs. 7 and 6). In addition, the copolymer irradiated with 4 Mrad reached a balance between swelling and dissolution earlier than the unirradiated copolymer, and at some point the dissolution mechanism took over. Further irradiation up to 10 Mrad produced a significant change in the initial slope and no plateau value was seen, which is indicative of major degradation. The correlation coefficient for the regression line plotted in this figure was 0.972.

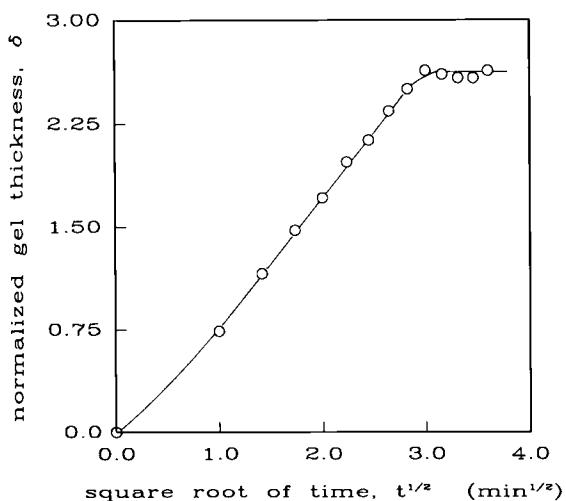


Fig. 6. Normalized gel thickness as a function of the square root of solvent diffusion time for MEK dissolution of P(MMA-co-MAH) slabs containing 0.60 molar fraction of MMA.

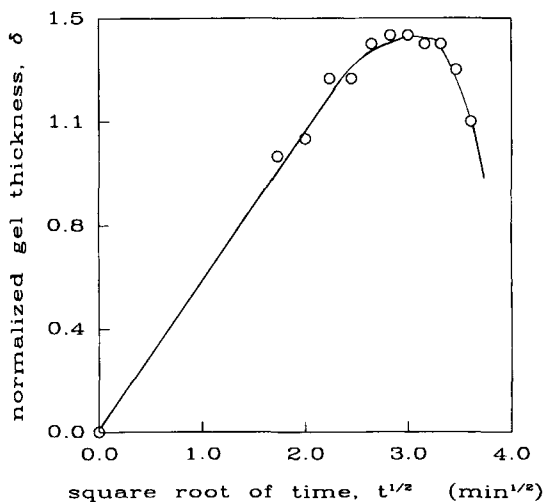


Fig. 7. Normalized gel thickness as a function of the square root of solvent diffusion time for MEK dissolution of P(MMA-co-MAH) slabs containing 0.60 molar fraction of MMA and irradiated with 4 Mrad.

Similar data were obtained for copolymers with 0.40 and 0.80 MMA. All results are summarized in Table II. It can be seen that the normalized gel thickness decreased with increasing radiation dose (due to increased dissolution rate over swelling rate). In addition, the slope of δ vs. $t^{1/2}$ curves and the initial dissolution rate decreased with increasing radiation dose.

As discussed before,¹¹ these overall dissolution processes consist of a swelling mechanism (phenomenon) which predominates at the beginning of the experiment and a *true* dissolution phenomenon which prevails towards the end. To

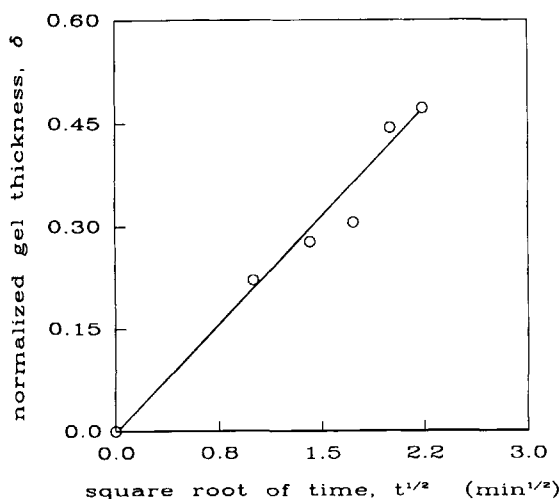


Fig. 8. Normalized gel thickness as a function of the square root of solvent diffusion time for MEK dissolution of P(MMA-co-MAH) slabs containing 0.60 molar fraction of MMA and irradiated with 10 Mrad.

TABLE II
Dissolution Characteristics of P(MMA-co-MAH) Copolymers

Mole fraction of MMA	Radiation dose (Mrad)	Normalized gel thickness at the plateau δ (Å)	Initial slope of dissolution curve ($\text{min}^{-1/2}$)	Initial dissolution rate (mm/min)
0.40	0	1.41	0.68	0.43
0.40	4	1.30	0.48	0.23
0.40	10	1.10	0.47	0.19
0.60	0	2.62	0.84	0.26
0.60	4	1.43	0.53	0.16
0.60	10	0.46	0.19	0.07
0.80	0	No plateau	0.30	0.17
0.80	4	No plateau	0.27	0.16

show this behavior, the data of Figure 5 were used to calculate the overall dissolution rate at various times during the process. The results of this analysis are shown in Figure 9. Positive overall rates indicate that the swelling rate is greater than the chain disentanglement/dissolution rate. Negative rates indicate that the disentanglement rate is greater than the swelling rate. Rates of zero correspond to the plateaus observed in Figure 5. Such results can be compared to the conclusions of Manjkow et al.,⁶ which show a similar behavior.

Mechanistic Analysis

Further analysis of the data of Figures 5–8 was conducted using the recently developed dissolution model of Lee and Peppas.¹¹ According to this analysis, the early portion of the overall dissolution process, which is domi-

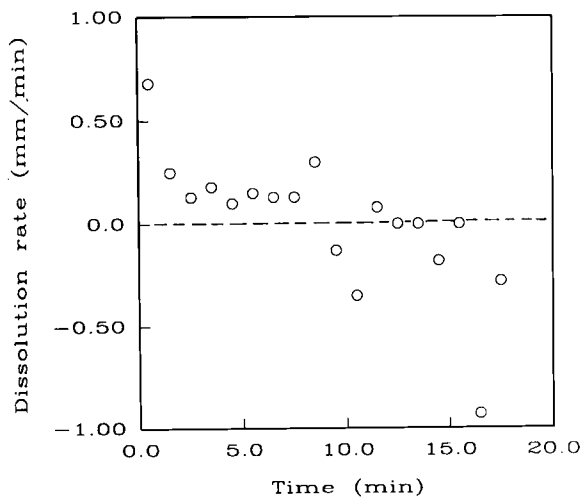


Fig. 9. Dissolution rate of sample appearing in Figure 5 as a function of time.

TABLE III
Analysis of P(MMA-co-MAH) Dissolution Data in MEK at 26°C
using the Lee and Peppas Model¹¹

Copolymer molar fraction of MMA	Irradiation dose (Mrad)	$\frac{(2 - c^*)(c^* - c_d)}{(1 - c^*)}$	Dissol. polym. volume fraction c_d (when $c^* = 0.975$)
0.40	0	36.63	0.08
	4	30.00	0.24
	10	14.91	0.61
0.60	0	53.07	-0.32
	4	14.98	0.61
	10	2.44	0.92
0.80	0	2.93	0.90
	4	3.65	0.89

nated by the swelling of the glassy polymer could be described by

$$\delta \approx \left(\frac{2(2 - c^*)(c^* - c_d)D_1^V t}{(1 - c^*)a^2} \right)^{1/2} \quad (1)$$

Here, δ is the normalized gel thickness, a is the half-thickness of the original slab, D_1^V is the MEK diffusion coefficient in the copolymer, and t is the diffusion time. The two dimensionless volume fractions, c^* and c_d , refer to the swelling agent volume fraction at the rubbery/glassy interface of the slab and the equilibrium polymer volume fraction at the dissolution front, respectively.

For the analysis of the P(MMA-co-MAH) data, the values of a , δ , and t were known, and the diffusion coefficient D_1^V was assumed to be 1×10^{-6} cm²/s, i.e., close to values reported¹⁶ for MEK diffusion in pure PMMA. Thus, the ratio $(2 - c^*)(c^* - c_d)/(1 - c^*)$ was calculated from the figures as reported in Table III. The value of c^* was not readily available for these systems. However, assuming $c^* = 0.975$, we were able to calculate the dissolution volume fraction of polymer, c_d , as reported in Table III.

It is interesting to note that as the irradiation dose increased, the dissolution polymer volume fraction increased, indicating that a smaller amount of MEK was necessary for the initial dissolution process. This is to be expected, since degraded copolymer chains are, in general, more soluble in MEK.

CONCLUSIONS

P(MMA-co-MAH) samples used as positive resists were investigated as to their dissolution behavior in methyl ethyl ketone. It was shown that the dissolution process is a function of radiation dose. This process starts with a swelling phenomenon of the glassy polymeric slab by water which is followed by chain disentanglement and true dissolution. If the swelling rate is greater than the dissolution rate, then the gel thickness increases linearly with square root of time. If the dissolution rate is greater than the swelling rate, then the gel thickness decreases with time.

References

1. L. F. Thompson, C. G. Wilson, and J. M. J. Fréchet, Eds., *Materials for Microlithography*, ACS Symposium Series, Vol. 266, Am. Chem. Soc., Washington, DC, 1984.
2. L. F. Thompson, C. G. Wilson, and M. J. Bowden, Eds., *Introduction to Microlithography*, ACS Symposium Series, Vol. 219, Am. Chem. Soc., Washington, DC, 1983.
3. A. C. Ouano, Y. O. Tu, and J. A. Carothers, in *Structure-Solubility Relationships in Polymers*, F. W. Harris and R. B. Seymour, Eds., Academic, New York, 1977, p. 11.
4. Y. O. Tu and A. C. Ouano, *IBM J. Res. Dev.*, **21**, 131 (1977).
5. A. C. Ouano, *Polym. Eng. Sci.*, **18**, 306 (1978).
6. J. Manjkow, J. S. Papanu, D. S. Soong, D. W. Hess, and A. T. Bell, *J. Appl. Polym. Sci.*, **62**, 682 (1987).
7. Y. M. N. Namaste, S. K. Obendorf, C. C. Anderson, P. D. Krasicky, and F. Rodriguez, *J. Vac. Sci. Technol.*, **B1**, 1160 (1983).
8. P. D. Krasicky, R. J. Groele, and F. Rodriguez, *J. Appl. Polym. Sci.*, **35**, 641 (1988).
9. E. E. Parsonage, N. A. Peppas, and P. I. Lee, *J. Vac. Sci. Technol.*, **B5**, 538 (1987).
10. E. E. Parsonage and N. A. Peppas, *Br. Polym. J.*, **19**, 469 (1987).
11. P. I. Lee and N. A. Peppas, *J. Controlled Release*, **6**, 207 (1987).
12. R. S. Harland, A. Gazzaniga, M. E. Sangalli, P. Colombo, and N. A. Peppas, *Pharmaceut. Res.*, **5**, 488 (1988).
13. M. C. deWilde and G. Smets, *J. Polym. Sci.*, **5**, 253 (1950).
14. C. M. Hansen, *Ind. Eng. Chem., Prod. Res. Dev.*, **8**, 2 (1969).
15. D. W. van Krevelen, *Properties of Polymers*, Elsevier, Amsterdam, 1976.
16. D. H. Hwang and C. Cohen, *Macromolecules*, **17**, 2890 (1984).

Received January 11, 1989

Accepted March 20, 1989